

Electronic properties and optical-absorption spectra of GaAs-Al_xGa_{1-x}As quantum wells in externally applied electric fields

G. D. Sanders

Universal Energy Systems, Inc., 4401 Dayton-Xenia Road, Dayton, Ohio 45432

K. K. Bajaj

*Avionics Laboratory, U.S. Air Force Wright Aeronautical Laboratories (AFWAL/AADR),
Wright-Patterson Air Force Base, Ohio 45433*

(Received 16 June 1986; revised manuscript received 24 October 1986)

A study of the electronic and optical properties of GaAs-Al_xGa_{1-x}As quantum wells in external electric fields is presented using a theory which incorporates valence-subband-mixing effects. Electric-field-induced changes in the conduction- and valence-subband structure, exciton binding energies, exciton oscillator strengths of both allowed ($\Delta n = 0$) and forbidden ($\Delta n \neq 0$) transitions, and the total absorption spectrum are calculated. Optical transitions associated with several conduction and valence subbands are considered. Computed electronic and optical properties are found to be the result of an interplay between the effects of the overlap of electron and hole envelope wave functions and the valence-subband mixing. Valence-subband mixing results in a large splitting of the Kramer's degeneracy in a quantum-well system in the presence of an electric field. The electric-field-induced changes in the computed exciton binding energies and oscillator strengths are caused mainly by the variation of the degree of overlap between the electron and hole wave functions. The foregoing results are compared with those obtained assuming no valence-band-mixing effects and are shown to be both qualitatively and quantitatively different. A brief comparison of our results with available experimental data is presented.

I. INTRODUCTION

Recently, there has been great interest in the electronic and optical properties of single-quantum-well and multiple-quantum-well (MQW) structures in the presence of electric fields.¹⁻²⁴ Most of the attention has been focused on the case where the field is applied perpendicular to the plane of the quantum-well interfaces. Both photoluminescence and absorption studies have been done in these systems. Emission and absorption spectra associated with both the heavy-hole and the light-hole excitons have been observed. All the studies show that the transition energies of these excitons decrease as the applied electric field is increased. In addition, the lines become broader and the intensity decreases with the increasing field. The conduction- and hole-subband energies and the binding energies of excitons in GaAs-Ga_{1-x}Al_xAs quantum-well structures in the presence of an electric field have been calculated recently by several groups.^{18,25-29} In these calculations, it is assumed that the heavy- and light-hole subbands are decoupled and Dingle's³⁰ simple particle in a box description is valid. The results of these calculations are in qualitative agreement with the experimental data.

The interest in electro-absorptive effects in quantum-well structures is strongly motivated by their potential applications in a variety of electro-optic devices such as high-speed modulators,¹⁴ self-linearized modulators,⁷ wavelength selective detectors,¹³ and optically bistable switches.⁸ Thus, there exists a need for more accurate models of the electronic and optical absorption properties

of quantum wells in applied electric fields. In this paper, we report a calculation of the conduction- and valence-subband energies, exciton binding energies, exciton oscillator strengths of both the allowed ($\Delta n = 0$) and the forbidden ($\Delta n \neq 0$) transitions, and the total absorption spectra in GaAs-Ga_{1-x}Al_xAs quantum-well structures in the presence of an external electric field. We follow a variational approach and take into account the effects of heavy- and light-hole subband mixing. These effects were first studied by Schulman and Chang³¹ using a nearest-neighbor empirical tight-binding model. They showed that the mixing of heavy- and light-hole components in quantum wells can lead to a number of interesting phenomena not predicted by the simple particle in a box model of Dingle.³⁰ Most important among these are the predictions of many "forbidden" transitions³¹ which violate the $\Delta n = 0$ selection rule, and the discovery of "negative" hole masses for subbands which are strongly interacting at the zone center. In GaAs-Al_xGa_{1-x}As quantum wells, the prototype negative mass subband is the first light-hole subband which interacts strongly with the second heavy-hole subband. In the presence of an externally applied electric field, the particle in a box model does predict the existence of forbidden transitions due to the breakdown of orthogonality between electron and hole envelope functions. However, predictions of the exciton oscillator strengths of these transitions, based on the particle in a box model, as we shall see later, are not found to be accurate. We therefore emphasize that the inclusion of the valence-band mixing effects is absolutely essential for accurate predictions of oscillator strengths

and binding energies of excitons in these systems.

We use a model of hole confinement which is intermediate in complexity between the particle in a box model used by Dingle³⁰ and the empirical tight-binding model of Schulman and Chang.³¹ The multiband effective-mass method we use is based on an extension of the $\mathbf{k}\cdot\mathbf{p}$ method in bulk semiconductors to the case of thin films as first described by Nedorezov,³² and recently used in the study of quantum-well structures by Fasolino and Altarelli.³³ This approach has the virtue of being relatively simple and yet takes into account the important aspects of the strong valence-band mixing near the zone center. All results obtained by the tight-binding model for GaAs-Al_xGa_{1-x}As quantum wells are reproduced nearly exactly, provided that the band parameters give the same bulk heavy- and light-hole masses. Using this rather efficient and flexible effective-mass method, we calculate the electric-field-induced changes in the conduction- and valence-subband structure, exciton binding energies, exciton oscillator strengths of both allowed and forbidden transitions, and the total absorption spectra. We consider optical transitions associated with several conduction and valence subbands and find that their properties are a result of overlap of zone-center electron and hole envelope functions and valence-subband mixing. The results obtained including valence-subband mixing effects are compared with those obtained assuming no mixing and are shown to be both qualitatively and quantitatively different. Finally, we compare our results with the available experimental data.

II. THEORY

The effective-mass model treats electrons and holes separately. The effective-mass Hamiltonian for the spin- $\frac{1}{2}$ electron states is given by

$$H_{\sigma\sigma'} = \left[\frac{p^2}{2m_e^*} + V_e(z_e) - V_F(z_e) \right] \delta_{\sigma\sigma'}, \quad (1)$$

where σ labels the electron spin ($\sigma = \pm \frac{1}{2}$), m_e^* is the effective mass of the electron taken to be $0.067m_0$, $V_e(z_e)$ is the confining square well potential whose height is taken to be 60% of the band-gap mismatch between the GaAs wells and Al_xGa_{1-x}As barriers,³⁴ and $V_F(z_e)$ is the potential due to the electric field. In our variational model, we use $V_F(z_e) = -eFz_e \Theta(W/2 - |z_e|)$, where e is the charge on the electron, F is the electric field strength, and $\Theta(x)$ is a unit step function which cuts off the electric field potential at the edge of the well of width W . The cutoff is necessary in order to obtain a variational solution since in the absence of the cutoff there are no true bound states. Bastard *et al.*²⁵ have shown that if the field strength is not too large the states will have a long lifetime and can be considered quasibound. Long-lived quasibound states exist for any particle in a well if the field strength satisfies the inequality

$$eF \ll \frac{\hbar^2 q_0^3}{2m^* W^3}. \quad (2)$$

The characteristic dimensionless wave vector q_0 is given by

$$q_0^3 = \left[\frac{2m^* W^2}{\hbar^2} (V_0 - E_n) \right]^{3/2}, \quad (3)$$

where V_0 is the well depth, m^* is the effective mass, and E_n is the particle in a box energy. When Eq. (2) is satisfied, the wave function decays rapidly inside the barrier and errors introduced by the cutoff in electric field are small. For typical quantum well states $(V_0 - E_n)$ is considerably larger than E_n and Eq. (2) holds for $F \leq 100$ kV/cm.

The effective-mass Hamiltonian for the spin- $\frac{3}{2}$ hole is given by

$$H_{\nu\nu'} = T_{\nu\nu'} + [V_h(z_h) + V_F(z_h)] \delta_{\nu\nu'}, \quad (4)$$

where $\nu = -\frac{3}{2}, \dots, \frac{3}{2}$ labels the z component of the hole spin. The kinetic energy matrix $T_{\nu\nu'}$ is given in the limit of infinite spin-orbit splitting by the $\mathbf{k}\cdot\mathbf{p}$ expression of Luttinger and Kohn³⁵ with k_z replaced by the operator p_z/\hbar , $V_F(z_h)$ is the electric field potential discussed earlier, and $V_h(z_h)$ is a finite square potential for the holes whose height is taken to be 40% of the band-gap mismatch between the GaAs wells and Al_xGa_{1-x}As barriers.³⁴ For the Luttinger parameters, we adopt values of $\gamma_1 = 6.93$, $\gamma_2 = 2.15$, and $\gamma_3 = 2.81$.³⁶ For the total band-gap mismatch, we use $\Delta E_g = 1.15x + 0.37x^2$ eV, where x is the aluminum concentration in Al_xGa_{1-x}As.³⁷ In the effective-mass model for holes, the potential is diagonal in the basis used. For the case where $F=0$, it can be shown by comparison with detailed tight-binding studies that the off-diagonal components are small.³⁸ Strong coupling between heavy- ($\nu = \pm \frac{3}{2}$) and light- ($\nu = \pm \frac{1}{2}$) hole subbands results from the off-diagonal components of $T_{\nu\nu'}$.

In the envelope-function approximation, the free electron and hole states are

$$\psi_n^e(\mathbf{k}_{||}) = \sum_{\sigma} f_n^{\sigma}(z_e) U_0^{\sigma}(\mathbf{r}) e^{i\mathbf{k}_{||}\cdot\mathbf{r}}, \quad (5)$$

and

$$\psi_m^h(\mathbf{k}_{||}) = \sum_{\nu} g_m^{\nu}(\mathbf{k}_{||}, z_h) U_0^{\nu}(\mathbf{r}) e^{i\mathbf{k}_{||}\cdot\mathbf{r}}, \quad (6)$$

respectively, where $U_0^{\sigma}(\mathbf{r})$ and $U_0^{\nu}(\mathbf{r})$ are zone-center Bloch functions for electrons and holes, and $f_n^{\sigma}(z_e)$ and $g_m^{\nu}(\mathbf{k}_{||}, z_h)$ are the corresponding envelope functions.

The envelope functions and subband structure are obtained by solving the effective-mass equations:

$$\left[\frac{p^2}{2m_e^*} + V_e(z_e) - V_F(z_e) \right] f_n^{\sigma}(z_e) = E_n^n f_n^{\sigma}(z_e), \quad (7)$$

where

$$E_n^e(\mathbf{k}_{||}) = E_0^n + \frac{\hbar^2 k_{||}^2}{2m_e^*},$$

and

$$\sum_{\nu'} \{ H_{\nu\nu'}(\mathbf{k}_{\parallel}, p_z) + [V_h(z_h) + V_F(z_h)] \delta_{\nu\nu'} \} g_m^{\nu'}(\mathbf{k}_{\parallel}, z_h) \\ = E_m^h(\mathbf{k}_{\parallel}) g_m^{\nu}(\mathbf{k}_{\parallel}, z_h). \quad (8)$$

To solve Eqs. (7) and (8) variationally, we expand $f_n(z_e)$ and $g_m^{\nu}(\mathbf{k}_{\parallel}, z_h)$ as sums of Gaussian-type orbitals of the form $e^{-\beta z^2}$ and $z e^{-\beta z^2}$, where the exponents β are chosen to cover a broad physical range. Substituting these expansions for the envelope functions into effective mass Eqs. (7) and (8), reduces the problem to a generalized eigenvalue problem to be solved for the subband energies $E_n^e(\mathbf{k}_{\parallel})$ and $E_m^h(\mathbf{k}_{\parallel})$ and envelope-function expansion coefficients.

The free-electron and hole-carrier states interact through the Coulomb force to form excitons. The exciton

wave function is made up of linear combinations of direct products of quantum-well electron and hole eigenfunctions,

$$\psi_x = \sum_{n,m} \sum_{\mathbf{k}_{\parallel}} \sum_{\mathbf{k}'_{\parallel}} F_{nm}(\mathbf{k}_{\parallel}, \mathbf{k}'_{\parallel}) | \mathbf{k}_{\parallel}, n \rangle | \mathbf{k}'_{\parallel}, m \rangle, \quad (9)$$

where n and m are subband indices for electron and hole, respectively. It can be shown that the exciton envelope function satisfies a two-dimensional effective-mass equation. The envelope function is given by

$$F_{nm}(\mathbf{k}_{\parallel}, \mathbf{k}'_{\parallel}) = \delta(\mathbf{k}_{\parallel} + \mathbf{k}'_{\parallel}) G_{nm}(\mathbf{k}_{\parallel}),$$

where $G_{nm}(\mathbf{k}_{\parallel})$, the exciton-relative-motion envelope function, satisfies

$$[E_n^e(\mathbf{k}_{\parallel}) - E_m^h(\mathbf{k}_{\parallel})] G_{nm}(\mathbf{k}_{\parallel}) + \sum_{n',m'} \sum_{\mathbf{k}'_{\parallel}} V_{n'm'}^{nm}(\mathbf{k}_{\parallel}, \mathbf{k}'_{\parallel}) G_{n'm'}(\mathbf{k}'_{\parallel}) = E G_{nm}(\mathbf{k}_{\parallel}). \quad (10)$$

In this expression, $E_n^e(\mathbf{k}_{\parallel})$ and $E_m^h(\mathbf{k}_{\parallel})$ are the energies for the n th conduction and m th valence subbands and the Coulomb interaction term $V_{n'm'}^{nm}(\mathbf{k}_{\parallel}, \mathbf{k}'_{\parallel})$ is given by (within the effective-mass approximation)

$$V_{n'm'}^{nm}(\mathbf{k}_{\parallel}, \mathbf{k}'_{\parallel}) = \frac{-e^2}{\epsilon_0 |\mathbf{k}_{\parallel} - \mathbf{k}'_{\parallel}|} \int dz_e \int dz_h f_n^*(z_e) f_n(z_e) \sum_{\nu} g_m^{\nu*}(\mathbf{k}'_{\parallel}, z_h) g_m^{\nu}(\mathbf{k}_{\parallel}, z_h) e^{i|\mathbf{k}_{\parallel} - \mathbf{k}'_{\parallel}| |z_e - z_h|}. \quad (11)$$

Here, ϵ_0 is the static dielectric constant and $f_n(z_e)$ and $g_m^{\nu}(\mathbf{k}_{\parallel}, z_h)$ are the electron- and hole-envelope wave functions discussed previously. We adopt a two-band model keeping only one valence and one conduction subband. We further approximate

$$\sum_{\nu} g_m^{\nu*}(\mathbf{k}'_{\parallel}, z_h) g_m^{\nu}(\mathbf{k}_{\parallel}, z_h)$$

in Eq. (11) by its value at the zone center. This is a fairly good approximation since the dominating contribution in Eq. (10) comes from the $\mathbf{k}_{\parallel} \simeq \mathbf{k}'_{\parallel}$ term, and we find that $\sum_{\nu} |g_m^{\nu*}(\mathbf{k}'_{\parallel}, z_h)|^2$ is a smooth function of \mathbf{k}_{\parallel} , even though $g_m^{\nu}(\mathbf{k}_{\parallel}, z_h)$ varies quickly with \mathbf{k}_{\parallel} . This two-band model allows us to ignore Fano resonances³⁹ of high-lying excitons with the continuum levels of lower-lying excitons. We solve Eq. (10) variationally by expanding G_{nm} as a sum of Gaussians of the form $e^{-\beta z^2}$ with exponents chosen to cover a broad physical range. The exciton energies and envelope wave functions are then obtained by solving a generalized eigenvalue problem for the expansion coefficients. All of the matrix elements are evaluated numerically and, in particular, we use the computed free carrier band structures in the evaluation of the kinetic-energy matrix. The energy bands are nearly isotropic in the region of interest near the band edges and with this approximation, all the numerical integrals are one dimensional.

The band-to-band absorption is calculated using Fermi's golden rule. The absorption coefficient is given by⁴⁰

$$\alpha(\hbar\omega) = \frac{4\pi^2 e^2 \hbar}{n_0 c m_0^2} \left[\frac{1}{\hbar\omega} \right] \sum_{\mathbf{k}_{\parallel}} \sum_{n,m} | \hat{\epsilon} \cdot \mathbf{p}_{nm}(\mathbf{k}_{\parallel}) |^2 \\ \times \Delta_{nm} [E_m^h(\mathbf{k}_{\parallel}) - E_n^e(\mathbf{k}_{\parallel}) + \hbar\omega], \quad (12)$$

where the optical matrix element

$$\mathbf{p}_{nm}(\mathbf{k}_{\parallel}) = \langle \psi_m^h(\mathbf{k}_{\parallel}) | \mathbf{p} | \psi_n^e(\mathbf{k}_{\parallel}) \rangle. \quad (13)$$

Here, $\psi_m^h(\mathbf{k}_{\parallel})$ and $\psi_n^e(\mathbf{k}_{\parallel})$ are the valence- and conduction-subband wave functions, respectively, m_0 is the free-electron mass, n_0 is the refractive index, $\hat{\epsilon}$ is the polarization vector, and $\hbar\omega$ is the energy of the incident photons.

In Eq. (12), the energy conserving δ function is replaced by

$$\Delta_{nm} [E_m^h(\mathbf{k}_{\parallel}) - E_n^e(\mathbf{k}_{\parallel}) + \hbar\omega],$$

a Lorentzian function of half width Γ_{nm} , which mimics the effects of inhomogeneous broadening in multi-quantum-well structures due to variations in the individual well sizes. It has been demonstrated that, within the approximation of uncoupled valence subbands, the bulk Franz-Keldysh effect neglecting effects of Coulomb interaction is recovered within the formalism of the present band-to-band absorption calculation in the limit of an infinitely wide quantum well.⁴¹ Finally, to include the first-order Coulomb interaction effects on the computed

band-to-band absorption, we multiply by the two-dimensional Coulomb enhancement factor of Shinada and Sugano.⁴²

In the envelope-function approximation, the optical matrix elements $\mathbf{p}_{nm}(\mathbf{k}_{\parallel})$ are given by

$$\mathbf{p}_{nm}(\mathbf{k}_{\parallel}) = \sum_{v,\sigma} \int d\mathbf{r} U_0^{v*}(\mathbf{r}) \mathbf{p} U_0^{\sigma}(\mathbf{r}) \int_{-\infty}^{\infty} dz f_n^{\sigma}(z) g_m^{v*}(\mathbf{k}_{\parallel}, z). \quad (14)$$

The integral over \mathbf{r} involves the Bloch functions of the optical matrix elements between the s -like spin- $\frac{1}{2}$ conduction Bloch state $U_0^{\sigma}(\mathbf{r})$ and the p -like spin- $\frac{3}{2}$ Bloch state $U_0^{\nu}(\mathbf{r})$. We denote this integral by $\langle \nu | \mathbf{p} | \sigma \rangle$.

For the holes, the basis states are linear combinations of the p -like Bloch states x , y , and z given by

$$| + \frac{3}{2} \rangle = \frac{1}{\sqrt{2}} (|x\rangle + i |y\rangle) \alpha, \quad (15)$$

$$| + \frac{1}{2} \rangle = \frac{1}{\sqrt{6}} [(|x\rangle + i |y\rangle) \beta - 2 |z\rangle \alpha], \quad (16)$$

$$| - \frac{1}{2} \rangle = \frac{1}{\sqrt{6}} [(|x\rangle - i |y\rangle) \alpha + 2 |z\rangle \beta], \quad (17)$$

and

$$| - \frac{3}{2} \rangle = \frac{1}{\sqrt{2}} (|x\rangle - i |y\rangle) \beta, \quad (18)$$

where α and β are spin- $\frac{1}{2}$ functions.

The matrix elements of interest are of the form $\langle r | \mathbf{p} | \sigma \rangle$, where $r = x, y, z$. Using the symmetry properties of the point group O_h , we conclude that $\langle x | p_x | \sigma \rangle = \langle y | p_y | \sigma \rangle = \langle z | p_z | \sigma \rangle$ while all other matrix elements vanish.

The nonvanishing bulk optical matrix elements for p_x and p_z are

$$\langle \pm \frac{3}{2} | p_x | \pm \frac{1}{2} \rangle = \frac{1}{\sqrt{2}} \langle x | p_x | \sigma \rangle, \quad (19)$$

$$\langle \pm \frac{1}{2} | p_x | \mp \frac{1}{2} \rangle = \frac{1}{\sqrt{6}} \langle x | p_x | \sigma \rangle, \quad (20)$$

and

$$\langle \pm \frac{1}{2} | p_z | \pm \frac{1}{2} \rangle = \frac{2}{\sqrt{6}} \langle x | p_x | \sigma \rangle, \quad (21)$$

where the matrix element $\langle x | p_x | \sigma \rangle$ is a constant defined in Ref. 43. The matrix elements for p_y are calculated similarly.

In bulk semiconductors, the optical matrix element is a slowly varying function of \mathbf{k} and may safely be approximated by its value at $\mathbf{k} = 0$. This approximation has also been made by a number of authors in the study of superlattices and quantum wells.³⁰ The $\Delta n = 0$ selection rule for transitions between subbands is based on the fact that in the envelope function approximation $\mathbf{p}_{nm}(\mathbf{k}_{\parallel} = 0)$ vanishes unless $n = m$.³⁰ Furthermore, the absorption coefficient in this approximation is given by (apart from a constant factor)

$$\alpha(\hbar\omega) \sim \frac{2}{\hbar\omega m_0} \sum_{n,m} | \hat{\mathbf{e}} \cdot \mathbf{p}_{mn}(0) |^2 \delta_{nm} J_{nm}(\hbar\omega), \quad (22)$$

where $J_{nm}(\hbar\omega)$ is the joint density of states between valence subband m and conduction subband n . For two-dimensional parabolic subbands, $J_{nm}(\hbar\omega)$ is a step function.³⁰

It has been pointed out recently⁴⁴⁻⁴⁶ that for superlattices and quantum wells, the approximation $\mathbf{p}_{nm}(\mathbf{k}_{\parallel}) \simeq \mathbf{p}_{nm}(0)$ is a very poor one. We find that $\mathbf{p}_{nm}(\mathbf{k}_{\parallel})$ is rapidly varying even for small values of \mathbf{k}_{\parallel} because of the strong mixing of heavy- and light-hole states by the off-diagonal elements in the valence-band Hamiltonian $H_{vv'}$. Thus, it is necessary to retain the \mathbf{k}_{\parallel} dependence of $\mathbf{p}_{nm}(\mathbf{k}_{\parallel})$ in our analysis. Fortunately, we have found that the squared optical matrix elements $| \hat{\mathbf{e}} \cdot \mathbf{p}_{nm}(\mathbf{k}_{\parallel}) |^2$ and the energy bands $E_m^h(\mathbf{k}_{\parallel})$ and $E_n^e(\mathbf{k}_{\parallel})$ are nearly independent of the direction of \mathbf{k}_{\parallel} allowing us to make an isotropic approximation. The integration over \mathbf{k}_{\parallel} in the formula for the absorption coefficient is one dimensional in the isotropic approximation.^{45,46} Having obtained the exciton envelope wave function $G_{nm}(\mathbf{k}_{\parallel})$ and the optical matrix elements $\mathbf{p}_{nm}(\mathbf{k}_{\parallel})$, the exciton oscillator strength can be determined by

$$f_{nm} = \frac{2}{E_g m_0} \left| \sum_{\mathbf{k}_{\parallel}} G_{nm}(\mathbf{k}_{\parallel}) \hat{\mathbf{e}} \cdot \mathbf{p}_{nm}(\mathbf{k}_{\parallel}) \right|^2, \quad (23)$$

where E_g is the energy gap in bulk GaAs.

The absorption coefficient for the (nm) th exciton, α_{nm} is related to the oscillator strength by⁴⁰

$$\alpha_{nm} = \frac{4\pi^2 e^2 \hbar f_{nm}}{n_0 m_0 c W} \Delta(\hbar\omega - E_{nm}). \quad (24)$$

As in the case of the band-to-band absorption, the exciton linewidth is assumed to result from effects of inhomogeneous broadening.

III. DISCUSSION

A. Valence-subband structure

We have investigated the effect of an applied electric field F on the valence-subband structure of GaAs-Al_{0.25}Ga_{0.75}As quantum wells. The valence-subband structures of 100- and 200-Å wells for two different values of the electric field strength F are shown in Figs. 1 and 2.

The valence subband structure is found to be very complicated and some of the bands are seen to have negative zone-center effective masses. The complicated band structure is due to strong interactions between different subbands at nonzero values of \mathbf{k}_{\parallel} as a result of the mixing of heavy- and light-hole states by off-diagonal components of $H_{vv'}$. At $\mathbf{k}_{\parallel} = 0$, these off-diagonal components are zero and the heavy- and light-hole states are decoupled. At points away from the zone center, the increasing strength of the level repulsion interaction with \mathbf{k}_{\parallel} can give rise to strong nonparabolicities in the computed band structure. The bands are labeled after the pure heavy- and light-hole states at $\mathbf{k}_{\parallel} = 0$; HH m and LH m denote the m th heavy- and light-hole levels, respectively. The zero of energy is taken at the maximum of $V_h(z_h) + V_F(z_h)$ for holes and at the minimum of

$V_e(z_e) - V_F(z_e)$ for electrons. Thus, the field dependence of the GaAs band gap, which is spatially indirect, is given by $E_g = E_0 - We |F|$, where E_0 is the zero-field GaAs band gap of 1.52 eV at 0 K.

In the absence of an applied field, the inversion symmetry of the square-well potential causes the valence subbands to exhibit a twofold Kramer's spin degeneracy. In this case, two sets of degenerate states are obtained by changing the signs of the spin indices. The two sets of valence states exhibit parity symmetry (even $\frac{3}{2}$, odd $\frac{1}{2}$, even $-\frac{1}{2}$, odd $-\frac{3}{2}$) and (odd $\frac{3}{2}$, even $\frac{1}{2}$, odd $-\frac{1}{2}$, even $-\frac{3}{2}$). When an electric field is applied, the inversion symmetry of the hole potential is lost and as a result the twofold Kramer's degeneracy of the valence subbands is lifted. It has been shown⁴⁷⁻⁵⁰ that this lifting of the twofold spin degeneracy is due to the lack of inversion symmetry and the presence of spin-orbit coupling.

The upper and lower branches of the spin-split valence-subband levels as defined by energy levels near the zone center do not interact with each other as can be seen by numerous level crossings at large values of $k_{||}$. This can be seen explicitly by block diagonalizing the 4×4 Luttinger Hamiltonian into two 2×2 subblocks via a unitary transformation.^{49,50}

The zone-center energies of electrons and holes as functions of F are shown in Figs. 3 and 4 for 100- and 200-Å wells, respectively. The band edges for band-to-band absorption between a given pair of electron and hole subbands n and m is given by the simple relation $E_{nm} = E_g + E_n - E_m$, where E_n and E_m are the electron- and hole-subband energies shown in Figs. 3 and 4 and $E_g = E_0 - We |F|$ is the GaAs band gap. In the weak-field limit where $eFW \ll \hbar^2 \pi^2 / 2m^* W^2$, $V_F(z)$ is a small perturbation and the energies E_n and E_m may be evaluated by perturbation theory. To second order in perturbation theory, we have

$$E_n = E_n^0 + We |F| / 2 - \langle n | V_F | n \rangle - \sum_{l \neq n} \frac{|\langle n | V_F | l \rangle|^2}{E_n^0 - E_l^0}. \quad (25)$$

Here, $|n\rangle$ and $|l\rangle$ are zero-field envelope functions for CBn and CBl (where CB represents conduction band), E_n^0 and E_l^0 are the corresponding zone-center energies at zero field, and the sum extends over all values of l except $l = n$. Because V_F is an odd function, $\langle n | V_F | n \rangle$ vanishes and the first-order shift is just $We |F| / 2$. Similarly, E_m is given to second order by

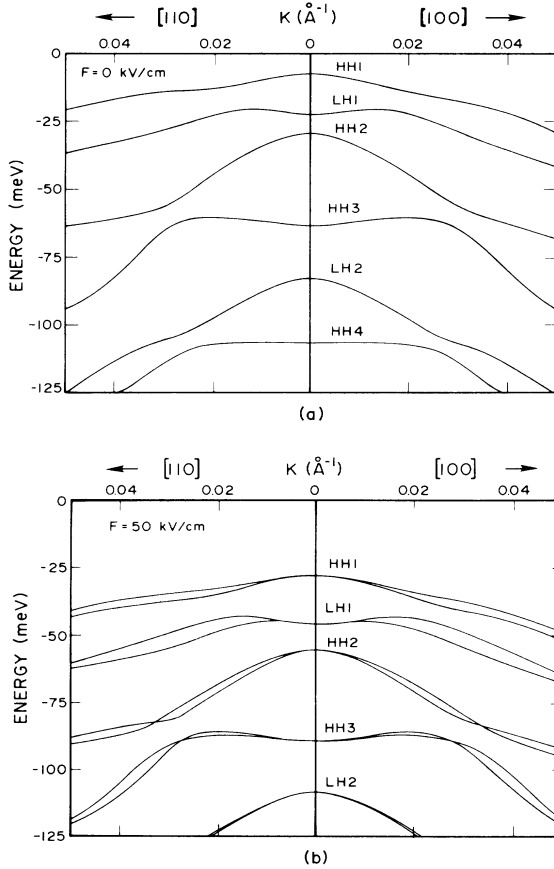


FIG. 1. Valence-subband structure for a 100-Å GaAs- $\text{Al}_{0.25}\text{Ga}_{0.75}\text{As}$ quantum well in an external electric field with (a) $F = 0$ kV/cm, and (b) $F = 50$ kV/cm.

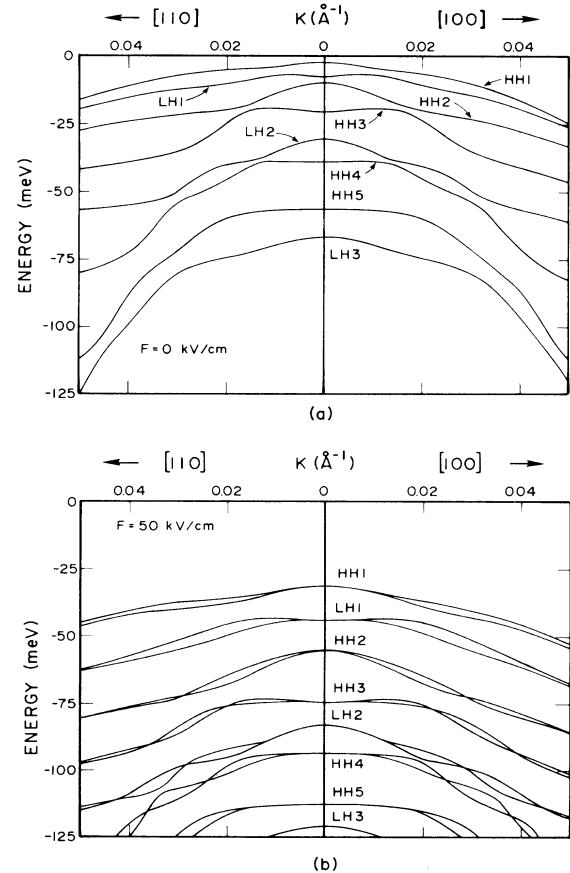


FIG. 2. Valence-subband structure for a 200-Å GaAs- $\text{Al}_{0.25}\text{Ga}_{0.75}\text{As}$ quantum well in an external electric field with (a) $F = 0$ kV/cm, and (b) $F = 50$ kV/cm.

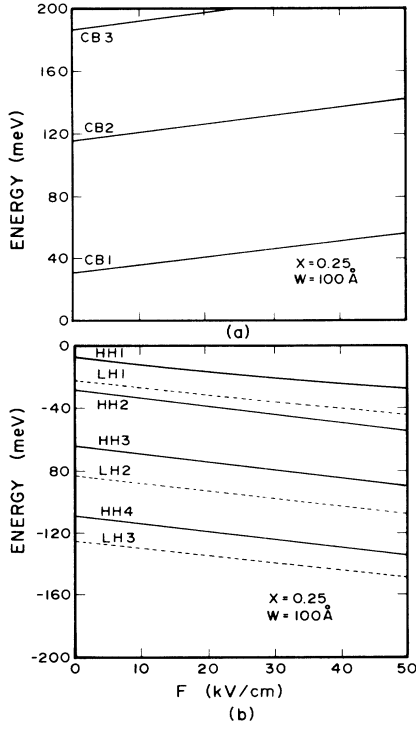


FIG. 3. Zone-center energies for (a) conduction and (b) valence subbands as functions of the applied external field F for a 100-Å GaAs-Al_{0.25}Ga_{0.75}As quantum well.

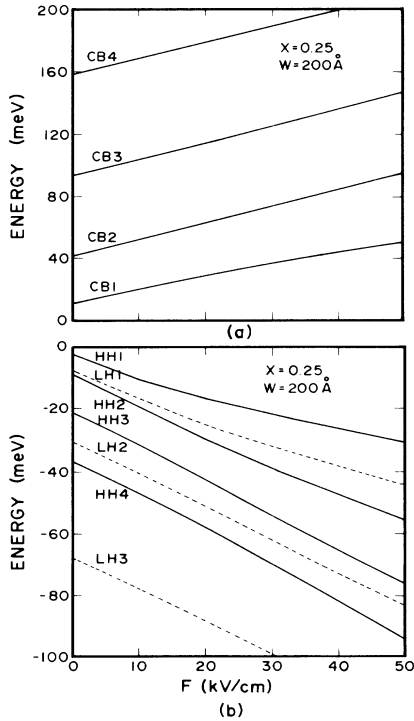


FIG. 4. Zone-center energies for (a) conduction and (b) valence subbands as functions of the applied external field F for a 200-Å GaAs-Al_{0.25}Ga_{0.75}As quantum well.

$$E_m = E_m^0 - We |F|/2 + \sum_l' \frac{|\langle m | V_F | l \rangle|^2}{E_m^0 - E_l^0}, \quad (26)$$

where now l and m refer to zone-center heavy- or light-hole envelope functions. Thus, the band-edge energies E_{nm} for band-to-band absorption are given by

$$E_{nm} = E_{nm}^0 - \sum_l' \frac{|\langle n | V_F | l \rangle|^2}{E_n^0 - E_l^0} + \sum_l' \frac{|\langle m | V_F | l \rangle|^2}{E_m^0 - E_l^0}, \quad (27)$$

where $E_{nm}^0 = E_0 + E_n^0 - E_m^0$. If we use infinite barrier envelope functions and energies, we can obtain the results of Bastard *et al.*²⁵ for $n = m = 1$, i.e.,

$$E_{1,1} = E_{1,1}^0 - C_0(m_e^* + m_h^*)e^2F^2W^2/\hbar^2, \quad (28)$$

where $C_0 = (1/24\pi^2)(15/\pi^2 - 1)$ and m_e^* and m_h^* are electron and hole masses along z . Thus, the second-order shift to lower energies of the HH1-CB1 and LH1-CB1 band-to-band absorption edges is proportional to the square of the well size and the sum of the carrier masses along the direction of confinement.

B. Exciton binding energy

The variation in the exciton binding energy as a function of electric field is shown in Figs. 5 and 6 for 100- and 200-Å GaAs-Al_{0.25}Ga_{0.75}As quantum wells. Although the detailed variation of the exciton binding energy with electric field is seen to be quite complicated, a qualitative picture is easily found.

The exciton kinetic energy for relative motion in Eq. (10) is determined by the joint density of states between valence and conduction subbands while the exciton potential energy is determined by the degree of overlap between the z -dependent charge densities of the particle in a box electron and hole envelope wave functions

$$-e |f_n(z_e)|^2$$

and

$$e \sum_v |g_m^v(z_h, 0)|^2.$$

The lifting of the Kramer's degeneracy results in the formation of closely spaced pairs of excitons having slightly different binding energies. The excitons associated with the upper branches of the hole subband curves near $\mathbf{k}=0$ have the larger binding energies since the upper branches of the valence subbands have the larger joint densities of states near the zone center. As mentioned previously, the 4×4 Luttinger Hamiltonian can be block diagonalized into 2×2 subblocks. Consequently, the two closely spaced pairs of excitons belong to two independent sets of excitons and do not interact with each other.

The variation in zone-center effective masses is fairly small so that the kinetic energy is a slowly varying function of the electric field. The potential energy, on the other hand, is rapidly varying due to strong perturbations in the envelope functions $f_n(z_e)$ and $g_m^v(z_h, 0)$. The electron is pushed against the direction of the applied field while

the hole is pushed in the opposite direction so that for strong enough fields the electron and hole charge densities are concentrated near opposite walls of the quantum well. For the HH1-CB1 and LH1-CB1 excitons whose z -dependent electron and hole charge densities have a single maximum at $z=0$ in the absence of the field, the application of a strong electric field results in a separation of charge density and a uniform decrease in the exciton potential energy and hence the binding energy. For excitons such as HH3-CB1, the story is somewhat different. In the absence of a field, the CB1 z -dependent charge density has a single maximum at $z=0$, the HH3 charge density has three maxima, and the largest contribution to the potential energy comes from the Coulomb interaction between the electron and hole charge densities concentrated at $z=0$. When a strong field is applied, the potential energy initially decreases as the electron and hole charge densities at $z=0$ are separated but then increases for a time before beginning a uniform decline when the electron charge density overlaps significantly with one of the secondary maxima of the HH3 charge density. Similar reasoning can be applied to other excitons to obtain a qualitative understanding of the variation in binding energy with electric field.

C. Exciton oscillator strength

We have also studied the oscillator strength for excitonic absorption as a function of the applied electric field in GaAs-Al_{0.25}Ga_{0.75}As quantum wells. We consider excitonic absorption for the usual experimental situation where unpolarized light is incident along the growth direction [i.e., (x,y) polarization]. For the case of a 100-Å quantum well, oscillator strengths for excitonic transitions for several prominent excitons to the first and second conduction subbands are shown in Figs. 7(a) and 7(b), respectively. For a 200-Å well, the oscillator strengths for excitonic transitions to the first two conduction subbands are shown in Figs. 8(a) and 8(b). The curves corresponding to excitons formed from upper and lower valence-subband levels are labeled by the letters u and l , respectively.

Referring to the figures, the oscillator strength curves are nontrivial and at first sight surprising. The detailed dependence of the oscillator strength on electric field can be viewed as a complicated interplay between the mixing of even- and odd-parity wave functions by the applied electric field for each of the heavy- and light-hole component wave functions and the mixing between heavy and

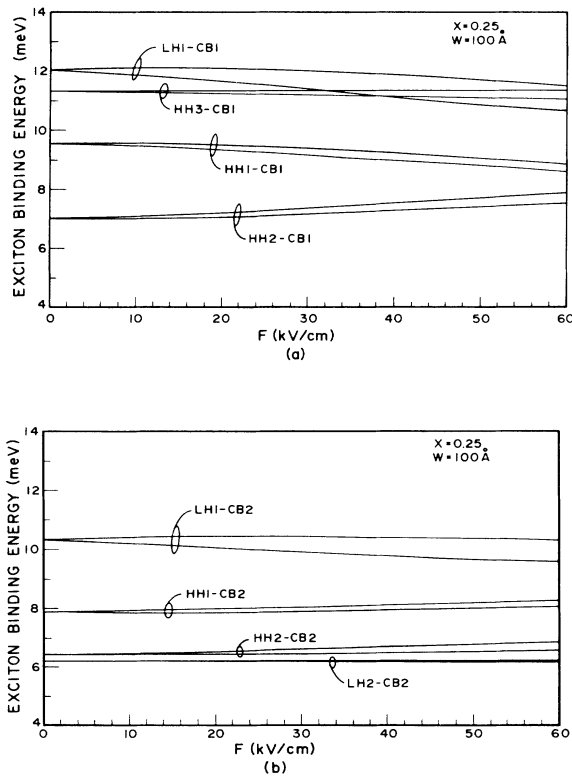


FIG. 5. Exciton binding energies for several prominent excitons as a function of applied electric field F for a 100-Å GaAs-Al_{0.25}Ga_{0.75}As quantum well for (a) excitonic transitions to the first conduction band and (b) excitonic transitions to the second conduction band.

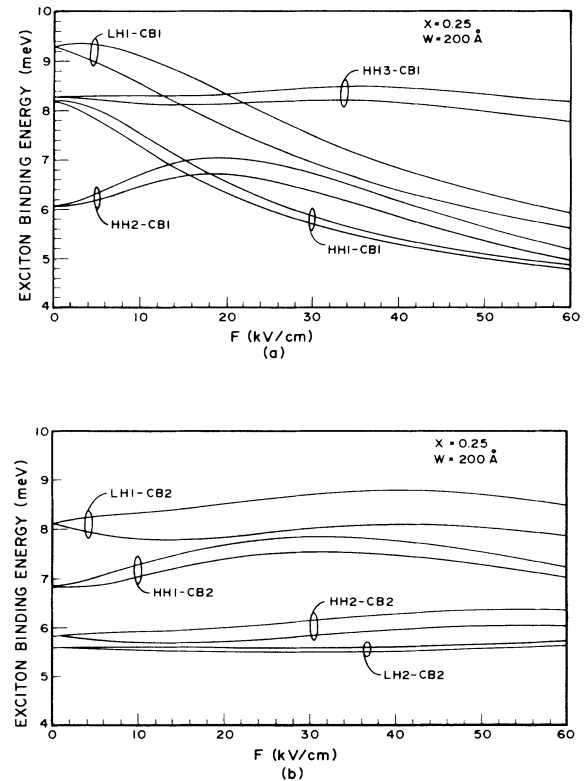


FIG. 6. Exciton binding energies for several prominent excitons as a function of applied electric field F for a 200-Å GaAs-Al_{0.25}Ga_{0.75}As quantum well for (a) excitonic transitions to the first conduction band and (b) excitonic transitions to the second conduction band.

light holes due to the off-diagonal components of the hole kinetic energy operator T_{vv} .

The major factor determining the oscillator strength for both allowed $\Delta n = 0$ and forbidden $\Delta n \neq 0$ excitons in an electric field is the mixing of even- and odd-parity wave functions by the applied electric field. To interpret the results of the detailed calculation, we first note that we may simplify Eq. (23) by supposing the exciton wave function $G_{nm}(k_{\parallel})$ to be a cap function with a cutoff for $|k_{\parallel}| \geq k_0$. For k_0 very small (i.e., for shallow excitons), we have

$$f_{nm} \sim |\hat{\epsilon} \cdot \mathbf{p}_{nm}(0)|^2 \sim |\langle f_n^{\sigma}(z_e) | g_m^{\nu}(0, z_h) \rangle|^2.$$

Thus, the oscillator strength is proportional to the simple overlap between the free electron and hole zone-center envelope functions. Referring to Fig. 8(a), the decrease in oscillator strength for HH1-CB1 and LH1-CB1 for $F > 10$ kV/cm is due primarily to the reduction in overlap between CB1 and the HH1 and LH1 wave functions with the application of the electric field. For the case of the HH2-CB1 exciton, the application of an increasing electric field and the resultant distortion of the CB1 and HH2 wave functions increases the overlap until a maximum is reached near a point where the CB1 wave-function peak

coincides with a local maximum of the HH2 wave function. Thereafter, the overlap between HH2 and CB1 decreases and the wave functions are forced against opposite walls of the quantum well by the electric field. A similar analysis for other excitonic transitions can be made.

At zero electric field, the oscillator strengths of the forbidden excitons are due almost entirely to the sharing of their oscillator strengths with those of allowed excitons through mixing of the hole envelope functions. In particular, the strong LH1-CB2 exciton absorption observed at zero electric field has been shown to result from sharing of its oscillator strength with that of the HH2-CB2 exciton due to strong hybridization of the LH1 and HH2 wave functions.^{51,52} Thus, one can have a situation where the variation in the oscillator strength of a forbidden exciton is determined not by the changes in the simple zone-center wave-function overlap of the forbidden exciton in question, but rather by changes in the oscillator strength of the $\Delta n = 0$ allowed transition with which it is strongly mixed and by changes in the degree of this mixing. A particularly good example of this is seen in the variation of the LH1-CB2 exciton oscillator strength in the 200-Å well case. For $F < 10$ kV/cm, the total oscillator strength of the LH1-CB2 excitons decreases rapidly in response to a decrease in the oscillator strength of the HH2-CB2 exci-

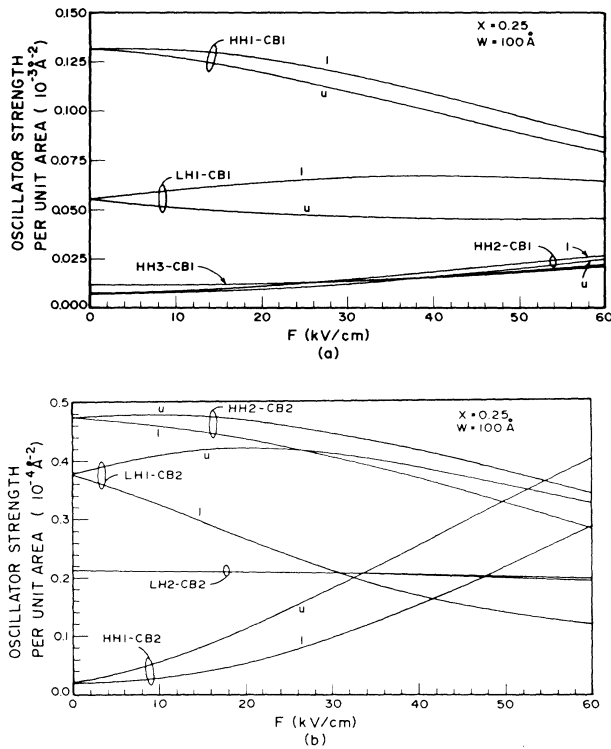


FIG. 7. Exciton oscillator strengths per unit area for several prominent excitons as a function of applied electric field F in a 100-Å GaAs-Al_{0.25}Ga_{0.75}As quantum well for (a) excitonic transitions to the first conduction band and (b) excitonic transitions to the second conduction band for unpolarized light incident along the growth direction.

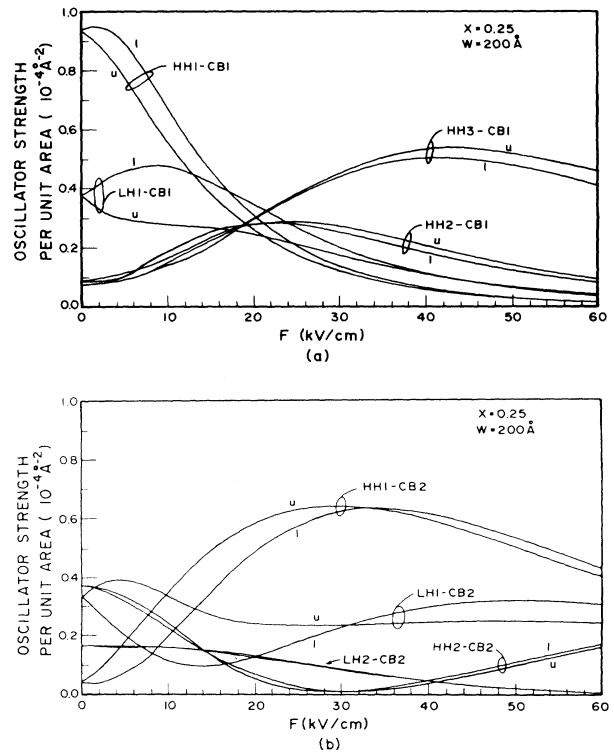


FIG. 8. Exciton oscillator strengths per unit area for several prominent excitons as a function of applied electric field F in a 200-Å GaAs-Al_{0.25}Ga_{0.75}As quantum well for (a) excitonic transitions to the first conduction band and (b) excitonic transitions to the second conduction band for unpolarized light incident along the growth direction.

tons with which they share oscillator strength and to variations in the degree of hybridization of HH2 and LH1. This decrease in the oscillator strength of the LH1-CB2 exciton occurs despite the fact that the simple zone-center overlap is an increasing function of electric field in the weak-field regime. Likewise the initial increase in the oscillator strength of the allowed LH1-CB1 exciton with electric field can also be explained as a mixing effect. The oscillator strength of LH1-CB1 grows in the weak-field regime by regaining the oscillator strength it shared with HH2-CB1 despite the fact that the zone-center overlap between LH1 and CB1 is a monotonically decreasing function of the electron field strength.

D. Exciton binding energy and oscillator strength in the uncoupled valence-band approximation

Many authors like to make calculations in which valence-subband mixing between light and heavy holes is neglected. A question arises as to the validity of this approach.

For the sake of completeness, we have also calculated exciton binding energies and oscillator strengths as a function of applied electric field for the 200-Å quantum well in an uncoupled valence-subband model for purposes of comparison with the present calculations. This is equivalent to retaining only the diagonal components in the kinetic-energy operator T_{vv} . In this picture, there is no coupling between heavy- and light-hole states and the valence subbands are all parabolic and the joint densities of states are all step functions. There is no lifting of the Kramer's degeneracy in this approximation. Furthermore, the optical matrix elements p_{nm} in this decoupled approximation are constants independent of $k_{||}$.

The computed exciton binding energies in the decoupled approximation are shown in Fig. 9. Comparing the results of the uncoupled bands model in Fig. 9 with the more realistic results shown in Fig. 6, we see that inclusion of mixing-induced valence-band nonparabolicity effects can change the computed exciton binding energy by 1–2 meV. The variations in exciton binding energy with electric field in the uncoupled approximation are due entirely to variations in the exciton potential energy.

The computed exciton oscillator strengths in the uncoupled valence-subband model are shown in Fig. 10. A factor of 2 has been included to account for spin degeneracy. In comparing these results with the more realistic calculation, one adds together the oscillator strengths of the spin-orbit split excitons. The results of the uncoupled valence-subband model are in fair agreement with results obtained using the more realistic valence-subband coupling model as can be seen by comparing Fig. 10 and Fig. 8. The simple overlap between free-electron and hole zone-center envelope functions, which determines the oscillator strength, is insensitive to nonparabolicity effects. In the weak-field limit, on the other hand, mixing effects are very important. In the decoupled bands model, the oscillator strengths of the forbidden excitonic transitions vanish at zero electric field while in the mixing calculation strong forbidden transitions are predicted due to the sharing of oscillator strengths between allowed and for-

bidden transitions. As mentioned earlier, the LH1-CB2 exciton oscillator strength for weak fields is derived from that of the HH2-CB2 exciton. In the uncoupled calculation at $F=0$ kV/cm, the HH2-CB2 oscillator strength is therefore approximately equal to the sum of oscillator strengths for the HH2-CB2 and LH1-CB2 excitons as calculated in the mixing model.

E. Computed absorption spectra

To facilitate comparison of our theoretical studies with experimental measurements, we have generated artificial absorption spectra to show the effect of an applied electric field on the absorption spectra of 100- and 200-Å GaAs-Al_{0.25}Ga_{0.75}As quantum wells. Computed absorption spectra for 100-Å quantum wells are shown in Fig. 11, and similar absorption spectra for a 200-Å quantum well are shown in Fig. 12. In the 100-Å cases, the band-to-band and excitonic linewidths Γ_x and Γ_b are given by $\Gamma=1n_en_h$ meV, where n_e and n_h are principal quantum numbers for electrons and holes. For the 200-Å well cases, $\Gamma=0.5n_en_h$ meV. The upper curves are the computed total absorption spectra and the lower curves are the band-to-band absorption spectra including the free excitonic absorption due to the Coulomb enhancement factor of Shinada and Sugano.⁴²

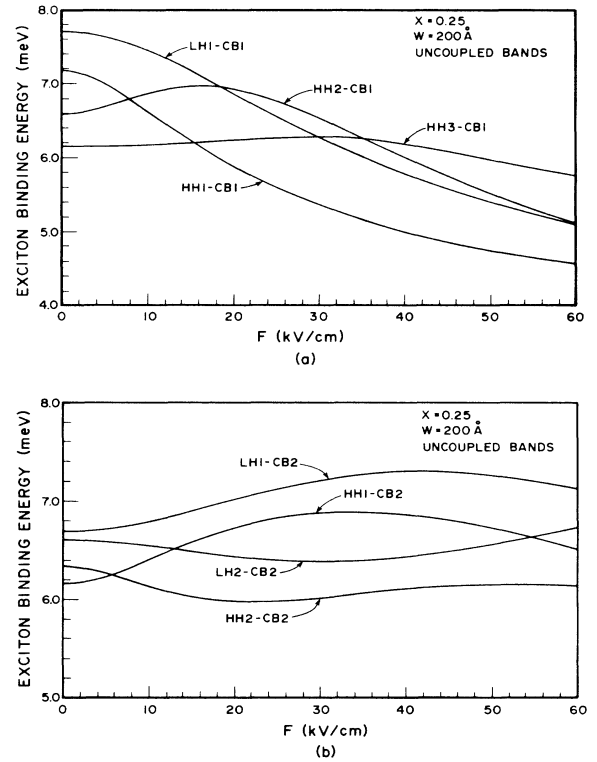


FIG. 9. Exciton binding energies in the uncoupled valence-bands approximation as a function of applied electric field F for a 200-Å GaAs-Al_{0.25}Ga_{0.75}As quantum well for (a) excitonic transitions to the first conduction band and (b) excitonic transitions to the second conduction band.

For a given electric field strength, the changes induced in the computed absorption spectra are more pronounced for wider quantum wells. In Fig. 11, we have the computed absorption of a 100-Å quantum well; Fig. 11(a) in the absence of an electric field and Fig. 11(b) in the applied field of 30 kV/cm. Over this range of electric field strength, the changes in the absorption coefficient are relatively minor. The onset of the band-to-band and HH1-CB1 excitonic absorption in an applied field of 30 kV/cm are both lowered by 1 meV, and the HH1-CB1 exciton peak is measurably weakened. The most interesting effect, however, is the shifting of oscillator strength from the LH1-CB2 forbidden exciton to the HH1-CB2 exciton, an effect which should be observable.

The computed absorption of a 200-Å quantum well for applied electric field strengths of 0, 10, 20, and 30 kV/cm is shown in Fig. 12 and the changes are seen to be much more pronounced. As the electric field strength increases, the oscillator strengths of the $\Delta n = 0$ allowed excitonic transitions decrease until at 30 kV/cm they are very weak. At the same time oscillator strength is transferred to the $\Delta n \neq 0$ transitions and at 30 kV/cm the most pronounced excitonic transitions are seen to be those involving states

with principal quantum numbers $n = 1$ and $n = 2$, i.e., HH2-CB1, HH1-CB2, and LH1-CB2. As discussed earlier, this is due primarily to the changes in the simple zone-center overlaps as the envelope functions are distorted by the electric field.

F. Comparison with experimental data

We now compare briefly our results with experimental data. As mentioned earlier, several groups have made emission as well as absorption measurements in GaAs-Al_xGa_{1-x}As multi-quantum-well structures in the presence of an electric field applied perpendicular to the plane of the structures. They all find that the energies associated with the lowest excitonic transitions, namely HH1-CB1 and LH1-CB1, decrease as a function of the applied electric field. Most of the decrease arises from the change in the conduction- and hole-subband energies and not from the change in the binding energies of the excitons. This is in general agreement with our results as can be seen from Figs. 3 and 5(a) for 100Å-wide GaAs quantum wells. Recently, Miller *et al.*¹⁸ have carried out a fairly detailed study of the effects of electric field on the optical absorption spectrum of a GaAs-Al_{0.32}Ga_{0.68}As multi-quantum-well structures with well and barrier sizes of 95 and 98 Å, respectively. They measure the energies of the absorption peaks associated with the heavy-hole

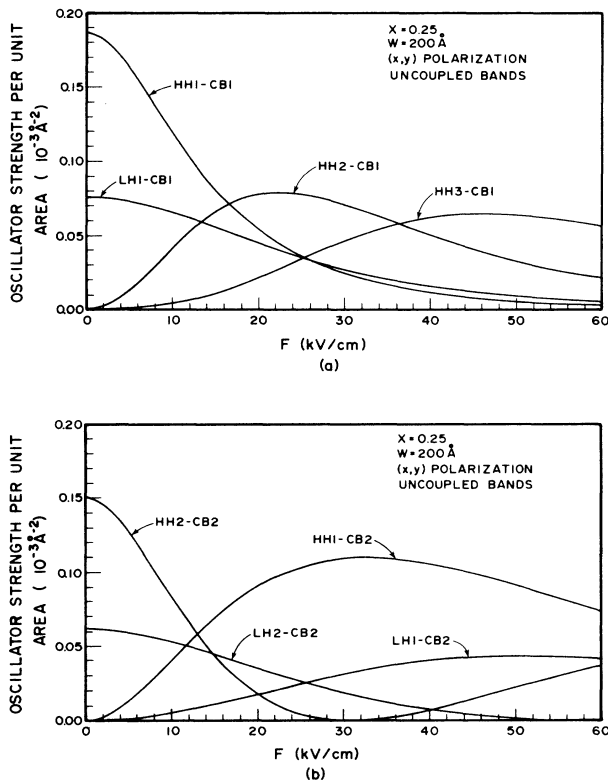


FIG. 10. Exciton oscillator strengths per unit area in the uncoupled valence-bands approximation for several prominent excitons as a function of applied electric field F in a 200-Å GaAs-Al_{0.25}Ga_{0.75}As quantum well for (a) excitonic transitions to the first conduction band and (b) transitions to the second conduction band for unpolarized light incident along the growth direction.

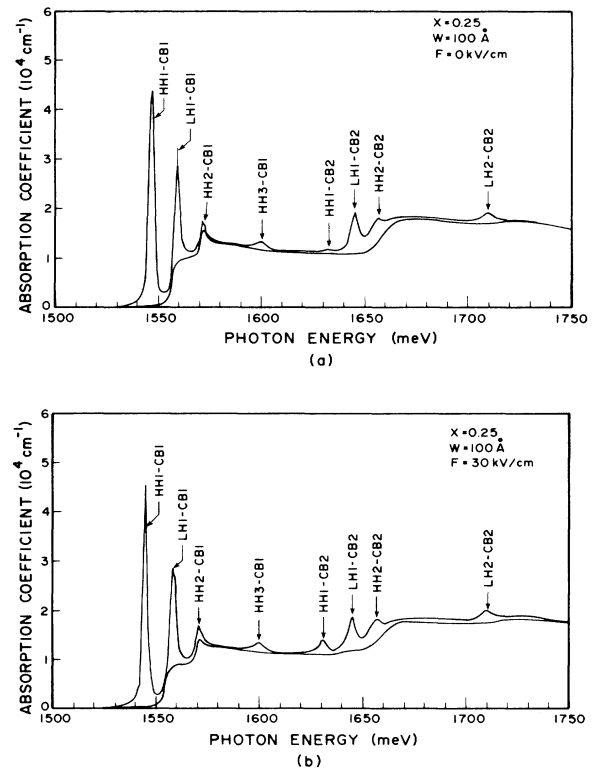


FIG. 11. Computed absorption spectra in a 100-Å GaAs-Al_{0.25}Ga_{0.75}As quantum well for unpolarized light incident along the growth direction. The applied electric field is taken to be (a) $F = 0$ kV/cm and (b) $F = 30$ kV/cm.

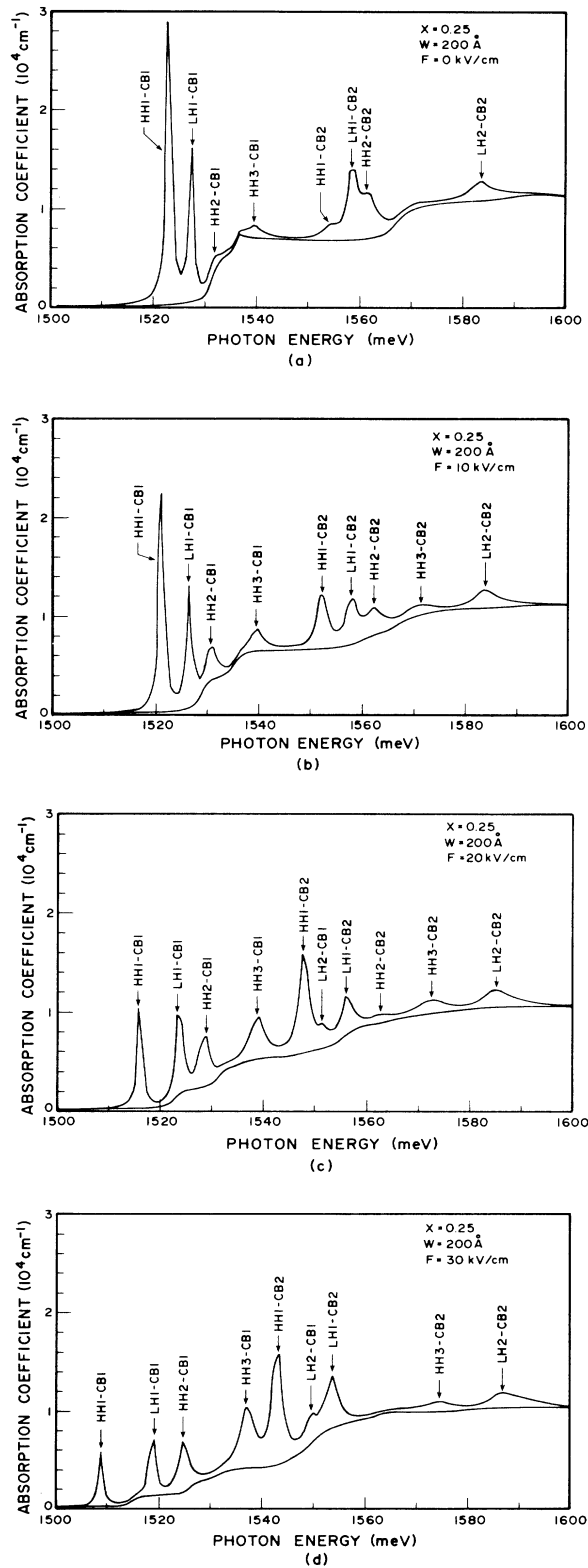


FIG. 12. Computed absorption spectra in a 200-Å GaAs-Al_{0.25}Ga_{0.75}As quantum well for unpolarized light incident along the growth direction. Applied electric field strengths are (a) $F = 0$ kV/cm, (b) 10 kV/cm, (c) 20 kV/cm, and (d) 30 kV/cm.

(HH1-CB1) and light-hole (LH1-CB1) excitons as a function of the applied electric field at room temperature and find that they decrease as the electric field is increased. They also calculate the positions of the lowest conduction and hole subbands and the binding energies of the heavy- and light-hole excitons as a function of the electric field using the decoupled valence band approximation. In their calculation, they assume a 57:43 band-gap discontinuity and use physical parameters first proposed by Miller *et al.*³⁴ Using the known value of the band gap of GaAs at room temperature (1.424 eV), and the calculated values of the subband and exciton binding energies, they determine the emission energies which agree quite well with the measured values. We have also calculated the energies of the conduction and valence subbands and the values of the exciton binding energies as a function of the electric field in 100-Å GaAs wells using the decoupled band approximation. As mentioned earlier, we use a 60:40 band-gap discontinuity rule and values of Luttinger parameters consistent with those proposed by Skolnick *et al.*³⁶ based on their cyclotron resonance work. These values are somewhat different from those used by Miller *et al.*¹⁸ We find that the position of the lowest conduction- and valence-subband levels we calculated, agree quite well with those calculated by Miller *et al.*¹⁸ and by Bastard *et al.*²⁵ keeping in mind that our well size (100 Å rather than 95 Å) and the Al concentration (0.25 rather than 0.32) are somewhat different. The values of the exciton binding energies we calculate, however, show a much smaller decrease as a function of the electric field than those calculated by Miller *et al.*¹⁸ The differences in the variation of the exciton binding energies with electric field are probably due to the use of different variational wave functions in the two calculations. In view of the uncertainties in determining the exact positions of the absorption peaks and the values of the various parameters of the multi-quantum-well structures, the agreement between our calculations and those of Miller *et al.*¹⁸ with the experimental data is quite good. Matsuura and Kamizato²⁸ have calculated the variations of the subband energies, exciton binding energies and exciton oscillator strengths as a function of the applied electric field in GaAs-Al_xGa_{1-x}As quantum wells assuming infinite potential barriers and using the decoupled band approximation. They follow a variational approach and consider excitons associated with two conduction subbands and two heavy- (light-) hole subbands. The variations they calculate agree with our results for the decoupled bands for large (> 100 Å) well sizes, where it is meaningful to compare the results of an infinite potential barrier calculation with ours. The effects of valence-subband mixing on the absorption energies of the excitons associated with the lowest bands are rather small. As discussed earlier, the inclusion of these effects leads to interesting and different predictions about the binding energies and the oscillator strengths of excitons associated with higher subbands in the presence of an applied electric field.

Recently, Collins *et al.*²³ and Yamanaka *et al.*²⁴ have independently studied the excitonic transitions in GaAs-Al_xGa_{1-x}As multi-quantum-well structures in the presence of an electric field applied perpendicular to the

growth direction using photocurrent spectroscopy. Both of these groups find a rich structure in their spectra and observe as many as eight transitions. As the value of the electric field is increased, these transitions shift toward lower energies and their relative strengths change. The behavior of their excitonic transitions is in agreement with the predictions of our theoretical model which takes into account the valence subband mixing. A detailed quantitative comparison between the absorption spectra we calculate and the spectra observed by these two groups is not possible as the experimental spectra are not normalized.

IV. SUMMARY AND CONCLUSIONS

In conclusion, we have studied the electronic and optical properties of 100- and 200-Å GaAs-Al_{0.25}Ga_{0.75}As quantum wells in an external electric field using a multi-band effective mass theory which takes valence-band-mixing effects into account. Computed electronic and op-

tical properties are found to be the result of a complicated interplay between envelope wave-function overlap effects and valence subband mixing. Electric-field-induced changes in these properties are dominated by changes in the overlap between electron and hole wave functions which govern the strength of the effective exciton potential. These results are compared with those obtained using decoupled valence subbands and also with experimental data.

ACKNOWLEDGMENTS

The authors acknowledge useful discussions with Professor Yia-Chung Chang of the University of Illinois at Urbana-Champaign and D. A. Broido of the Naval Research Laboratory in Washington, D.C. This work was funded under U.S. Air Force Contract No. F33601-82-C-1716.

- ¹D. A. B. Miller, D. S. Chemla, D. J. Eilenberger, P. W. Smith, A. C. Gossard, and W. T. Tsang, *Appl. Phys. Lett.* **41**, 679 (1982).
- ²E. E. Mendez, G. Bastard, L. L. Chang, L. Esaki, H. Morkoc, and R. Fischer, *Phys. Rev. B* **26**, 7101 (1982).
- ³D. S. Chemla, T. C. Damen, D. A. B. Miller, A. C. Gossard, and W. Wiegmann, *Appl. Phys. Lett.* **42**, 864 (1983).
- ⁴R. C. Miller and A. C. Gossard, *Appl. Phys. Lett.* **43**, 954 (1983).
- ⁵T. H. Wood, C. A. Burrus, D. A. B. Miller, D. S. Chemla, T. C. Damen, A. C. Gossard, and W. Wiegmann, *Appl. Phys. Lett.* **44**, 16 (1984).
- ⁶D. A. B. Miller, D. S. Chemla, T. C. Damen, A. C. Gossard, W. Wiegmann, T. H. Wood, and C. A. Burrus, *Phys. Rev. Lett.* **53**, 2173 (1984).
- ⁷D. A. B. Miller, D. S. Chemla, T. C. Damen, T. H. Wood, C. A. Burrus, A. C. Gossard, and W. Wiegmann, *Opt. Lett.* **9**, 567 (1984).
- ⁸D. A. B. Miller, D. S. Chemla, T. C. Damen, A. C. Gossard, W. Wiegmann, T. H. Wood, and C. A. Burrus, *Appl. Phys. Lett.* **45**, 13 (1984).
- ⁹J. A. Kash, E. E. Mendez, and H. Morkoc, *Appl. Phys. Lett.* **46**, 173 (1985).
- ¹⁰M. Yamanishi, Y. Kan, T. Minami, I. Suemune, H. Yamamoto, and Y. Usami, *Superlatt. Microstruc.* **1**, 111 (1985).
- ¹¹P. W. Yu, D. C. Reynolds, K. K. Bajaj, C. W. Litton, W. T. Masselink, R. Fischer, and H. Morkoc, *J. Vac. Sci. Technol. B* **3**, 624 (1984).
- ¹²J. S. Weiner, D. S. Chemla, D. A. B. Miller, T. H. Wood, D. Sivco, and A. Y. Cho, *Appl. Phys. Lett.* **46**, 619 (1985).
- ¹³T. H. Wood, C. A. Burrus, A. H. Gnauck, J. M. Wiesenfeld, D. A. B. Miller, D. S. Chemla, and T. C. Damen, *Appl. Phys. Lett.* **47**, 190 (1985).
- ¹⁴T. H. Wood, C. A. Burrus, D. A. B. Miller, D. S. Chemla, T. C. Damen, A. C. Gossard, and W. Wiegmann, *IEEE J. Quant. Electron.* **QE-21**, 117 (1985).
- ¹⁵J. S. Weiner, D. A. B. Miller, D. S. Chemla, T. C. Damen, C. A. Burrus, T. H. Wood, A. C. Gossard, and W. Wiegmann, *Appl. Phys. Lett.* **47**, 1148 (1985).
- ¹⁶Y. Horikoshi, A. Fischer, and K. Ploog, *Phys. Rev. B* **31**, 7859 (1985).
- ¹⁷H. Iwamura, T. Saku, and H. Okamoto, *Jpn. J. Appl. Phys.* **24**, 104 (1985).
- ¹⁸D. A. B. Miller, D. S. Chemla, T. C. Damen, A. C. Gossard, W. Wiegmann, T. H. Wood, and C. A. Burrus, *Phys. Rev. B* **32**, 1043 (1985).
- ¹⁹M. Yamanishi, Y. Usami, Y. Kan, and I. Suemune, *Jpn. J. Appl. Phys.* **24**, L586 (1985).
- ²⁰Y. Kan, M. Yamanishi, I. Suemune, H. Yamamoto, and T. Yao, *Jpn. J. Appl. Phys.* **24**, L589 (1985).
- ²¹Y. Horikoshi, A. Fischer, and K. Ploog, *Jpn. J. Appl. Phys.* **24**, 955 (1985).
- ²²M. Erman, P. Frijlink, J. B. Theeten, C. Alibert, and S. Gaillard, in *Proceedings of the International Symposium on GaAs and Related Compounds*, Inst. Phys. Conf. Proc. No. **74**, edited by B. de Cremoux (IOP, London, 1985), p. 327.
- ²³R. T. Collins, K. v. Klitzing, and K. Ploog, *Phys. Rev. B* **33**, 4378 (1986).
- ²⁴K. Yamanaka, T. Fukunaga, N. Tsukada, K. L. I. Kobayashi, and M. Ishii, *Appl. Phys. Lett.* **48**, 840 (1986).
- ²⁵G. Bastard, E. E. Mendez, L. L. Chang, and L. Esaki, *Phys. Rev. B* **28**, 3241 (1983).
- ²⁶J. A. Brum and G. Bastard, *Phys. Rev. B* **31**, 3893 (1985).
- ²⁷E. J. Austin and M. Jaros, *Appl. Phys. Lett.* **47**, 274 (1985).
- ²⁸M. Matsuura and T. Kamizato, *Phys. Rev. B* **33**, 8385 (1986).
- ²⁹T. Hiroshima and R. Lang, *Appl. Phys. Lett.* **49**, 639 (1986).
- ³⁰R. Dingle, in *Festkorperprobleme*, edited by H. J. Queisser (Pergamon, New York, 1975), Vol. 15, p. 21.
- ³¹J. N. Schulman and Y. C. Chang, *Phys. Rev. B* **24**, 4445 (1981).
- ³²S. S. Nedorezov, *Fiz. Tverd. Tela (Leningrad)* **12**, 2269 (1970) [*Sov. Phys.—Solid State* **12**, 1814 (1971)].
- ³³M. Altarelli, *Phys. Rev. B* **28**, 842 (1983); A. Fasolino and M. Altarelli, *Two Dimensional Systems, Heterostructures, and Superlattices* (Springer Verlag, New York, 1984), p. 176.
- ³⁴R. C. Miller, D. A. Kleinman, and A. C. Gossard, *Phys. Rev. B* **29**, 7085 (1984); W. I. Wang, E. E. Mendez, and F. Stern, *Appl. Phys. Lett.* **45**, 639 (1984); D. Arnold, A. Ketterson, T. Henderson, J. Klem, and H. Morkoc, *Appl. Phys. Lett.* **45**, 1237 (1984).
- ³⁵J. M. Luttinger and W. Kohn, *Phys. Rev.* **97**, 869 (1955).
- ³⁶M. S. Skolnick, A. K. Jain, R. A. Stradling, J. C. Ousset, and

- S. Askenasy, *J. Phys. C* **9**, 2809 (1976); these parameters were slightly adjusted within the experimental error to give better agreement between our predicted absorption spectra and the published experimental data at zero-field strength.
- ³⁷H. J. Lee, L. Y. Juravel, J. C. Wolley, and A. J. Springthorpe, *Phys. Rev. B* **21**, 659 (1980).
- ³⁸G. D. Sanders and Y. C. Chang (unpublished).
- ³⁹U. Fano, *Phys. Rev.* **124**, 1866 (1961).
- ⁴⁰See, for example, F. Bassani and C. P. Parravicini, *Electronic States and Optical Properties in Solids* (Pergamon, New York, 1975), Chap. 5.
- ⁴¹D. A. B. Miller, D. S. Chemla, and S. Schmitt-Rink, *Phys. Rev. B* **33**, 6976 (1986).
- ⁴²M. Shinada and S. Sugano, *J. Phys. Soc. Jpn.* **21**, 1396 (1966).
- ⁴³P. Lawaetz, *Phys. Rev. B* **4**, 3460 (1971).
- ⁴⁴J. N. Schulman and Y. C. Chang, *Phys. Rev. B* **31**, 2056 (1985).
- ⁴⁵Y. C. Chang and J. N. Schulman, *Phys. Rev. B* **31**, 2069 (1985).
- ⁴⁶G. D. Sanders and Y. C. Chang, *Phys. Rev. B* **31**, 6892 (1985).
- ⁴⁷E. Banghert, K. von Klitzing, and G. Landwehr, in *Proceedings of the Twelfth International Conference on the Physics of Semiconductors, Stuttgart, 1974*, edited by M. H. Pilkuhn (Teubner, Stuttgart, 1974), p. 714.
- ⁴⁸F. J. Ohkawa and Y. Uemura, *Suppl. Prog. Theor. Phys. Suppl.* **57**, 164 (1975).
- ⁴⁹U. Ekenberg and M. Altarelli, *Phys. Rev. B* **30**, 3569 (1984).
- ⁵⁰D. A. Broido and L. J. Sham, *Phys. Rev. B* **31**, 888 (1985).
- ⁵¹G. D. Sanders and Y. C. Chang, *Phys. Rev. B* **32**, 5517 (1985).
- ⁵²R. C. Miller, A. C. Gossard, G. D. Sanders, Y. C. Chang, and J. N. Schulman, *Phys. Rev. B* **32**, 8452 (1985).